

Pulsed second-harmonic generation in nonlinear, one-dimensional, periodic structures

M. Scalora,^{1,2} M. J. Bloemer,² A. S. Manka,³ J. P. Dowling,² C. M. Bowden,² R. Viswanathan,⁴ and J. W. Haus⁴

¹*Time Domain Systems, Inc., Suite 100, 6700 Odyssey Drive, Huntsville, Alabama 35806*

²*Weapons Sciences Directorate, AMSMI-RD-WS-ST, Research, Development, and Engineering Center, U.S. Army Missile Command, Redstone Arsenal, Alabama 35898-5248*

³*National Science Foundation, 4201 Wilson Blvd., Arlington, Virginia 22230*

⁴*Physics Department, Rensselaer Polytechnic Institute, Troy, New York 12180-3590*

(Received 16 December 1996; revised manuscript received 30 April 1997)

We present a numerical study of second-harmonic (SH) generation in a one-dimensional, generic, photonic band-gap material that is doped with a nonlinear $\chi^{(2)}$ medium. We show that a 20-period, 12- μm structure can generate short SH pulses (similar in duration to pump pulses) whose energy and power levels may be 2–3 orders of magnitude larger than the energy and power levels produced by an equivalent length of a phase-matched, bulk medium. This phenomenon comes about as a result of the combination of high electromagnetic mode density of states, low group velocity, and spatial phase locking of the fields near the photonic band edge. The structure is designed so that the pump pulse is tuned near the first-order photonic band edge, and the SH signal is generated near the band edge of the second-order gap. This maximizes the density of available field modes for both the pump and SH field. Our results show that the $\chi^{(2)}$ response is effectively enhanced by several orders of magnitude. Therefore, mm- or cm-long, quasi-phase-matched devices could be replaced by these simple layered structures of only a few micrometers in length. This has important applications to high-energy lasers, Raman-type sources, and frequency up- and down-conversion schemes.

[S1050-2947(97)09009-4]

PACS number(s): 42.65.Ky, 42.79.Nv, 41.20.Bt, 78.66.–w

I. INTRODUCTION

Recently, one-, two-, and three-dimensional periodic dielectric structures have attracted a great deal of attention in the optics community [1,2]. In such materials, electromagnetic field propagation is forbidden for a range of frequencies, and allowed for others. The nearly complete absence of some frequencies in the transmitted spectrum is referred to as a photonic band gap (PBG), in analogy to semiconductor band gaps [3]. This phenomenon is based on the interference of light; for frequencies inside the band gap, forward- and backward-propagating components can cancel destructively inside the structure, leading to complete reflection.

Two- and three-dimensional structures, in particular, have been the focus of many studies over the past few years. Here, however, we study the dynamics associated with ultrashort pulses (about 1 ps or less) in one-dimensional systems. One-dimensional structures are simple, and they often provide proof-of-principle results that are fundamental and that may be extended to higher dimensions; they can also be more easily fabricated to satisfy current technology needs. For example, some potential applications that have been highlighted recently are the prediction of optical limiting and switching of ultrashort pulses [4]; nonlinear optical diode behavior [5]; the photonic band-edge laser [6]; and (more recently) the theoretical prediction and the experimental verification of a tunable, optical true-time delay line [7]. In Ref. [7] we showed that a ps pulse could propagate undistorted through a 30-period GaAs/AlAs PBG crystal only 8 μm in length, with a tunable delay of 10–110 μm , making the delay-to-device length ratio greater than one order of magnitude. The predicted and measured minimum in the group velocity was of order $c/14$, where c is the speed of light in

vacuum. The PBG material acts like a medium whose index of refraction is 14. We remark that this is a linear effect that is entirely due to interference effects of light near the photonic band edge.

Previous investigations of nonlinear optical behavior in large-index modulation, one-dimensional PBG structures by other authors have focused on $\chi^{(3)}$ processes [8], such as optical switching and gap-soliton propagation. In this paper, we study the effects of propagation in a $\chi^{(2)}$ active medium. Although these nonlinear processes are of different order, it has been known for some time that second-order nonlinearities can lead to an effective nonlinear $\chi^{(3)}$ response, and large phase shifts in the fundamental beam [9]. Only recently, however, has the nature and extent of the phase shift been extensively studied theoretically and experimentally [10]. As a result, novel, lower-intensity approaches to all-optical switching that utilize second-order nonlinearities have been devised [11].

In part, this work was originally motivated by a recent issue of *Physics Today* [12], where several aspects of nonlinear optical interactions—including second-harmonic (SH) generation, materials, laser tunability, and conversion efficiencies—were all discussed. Recent and extensive literature that exists on SH generation [9–27] is evidence of the importance of the process; also important are frequency up- and down-conversion, and the more general issue of obtaining laser radiation at frequencies generally not accessible with a more direct process.

SH generation and enhancement in periodic structures was first suggested in the early 1970s [28]. Because of the phase mismatch between the fundamental and SH fields, optimal enhancement was predicted only for the reflected SH component. The idea is to introduce a periodic modulation of

the linear background index in order to induce a phase-matching condition for second harmonic generation. This can be accomplished in either a uniform Bragg grating geometry [29], or in a periodic structure with a defect mode [30,31] sometimes referred to as a Fabry-Pérot cavity mode; both approaches are qualitatively similar. Phase matching of SH waves is also possible in thin-film waveguides if a periodicity, or corrugation, is introduced in the film deposited on a substrate [32]. In general, however, cavity-enhancement schemes rely on creating a resonant cavity for either the pump or the second-harmonic field. In the first case, either field may be tuned near the band edge; in the case of a cavity with a defect mode, the resonant mode is found inside the photonic band gap, where a transmission resonance is created thanks to the introduction of a phase slip within the structure.

The first experimental demonstration of reflected SH generation enhancement was accomplished with counterpropagating beams in a 17-layer, GaAs-Al_xGa_{1-x}As, quarter-wave structure [33]. The quarter-wave condition was satisfied at $\lambda=2\ \mu\text{m}$. In the experiment, a 2- μm beam was up-converted to 1- μm radiation. The fundamental beam was tuned in the middle of the photonic band gap, where maximum pump reflection (about 70%) occurs. The higher-order gap was centered at approximately $\lambda=0.7\ \mu\text{m}$, and the SH signal was tuned in the middle of the pass band.

More recently, experimental observations of an enhanced SH signal have been reported in a vertical-cavity geometry composed of GaAs/AlAs layers, where 10%/W enhancement of gain with respect to bulk was observed in the undepleted-pump (or linear) regime [34]. The structure was optimized to confine the fundamental field efficiently, and hence provide increased SH gain. Also recently, experimental evidence of SH signal enhancement in a PBG structure with a Fabry-Pérot defect mode has been reported; these results also suggest order-of-magnitude enhancement of the SH signal [31].

Analytical results for the case of uniform, shallow Bragg gratings (index modulation depth less than 10^{-2}) with a resonant, plane-wave SH field indicate order-of-magnitude enhancement of SH generation near the band edge of a fiber grating [29]. However, significant enhancement is expected only for a narrow-frequency bandwidth because of the small index modulation depth. Also, numerical integrations of Maxwell's equations with boundary conditions that included a defect mode have been carried out [30] using the matrix transfer method. The authors assumed a resonant second-harmonic field, and only a forward-propagating pump. They did not consider pump reflections because the pump was assumed to be tuned away from any resonance or the band edge. This neglect is not valid in the case of deep-grating PBG structures, since inside the structure forward- and backward-propagating components can be very significant even away from the band edge. For example, we have shown that for an index modulation of order unity, the Poynting vector inside the structure contains forward- and backward-propagating components of nearly the same magnitude. At frequencies near the band edge, where the transmission may be unity [7], there are no reflected waves from the structure: multiple reflections inside the periodic structure must therefore be accounted for to all orders. Nevertheless, the authors of Ref. [30] also found order-of-magnitude enhancement of

the second-harmonic signal, in qualitative agreement with the results for SH enhancement in a uniform, shallow fiber grating.

In general, several procedures have been developed to analyze nonlinear wave mixing and harmonic generation in multilayered structures [35,36]. In Ref. [35], for example, the matrix transfer method is modified in order to take into account nonlinear polarization sources in the undepleted pump regime. In Ref. [36], a formalism that includes a combination of Green's functions [37] and the matrix transfer method is developed to handle plane-wave propagation in an arbitrary multilayer geometry. Our interest here is to extend the analysis of SH generation and enhancement to arbitrarily deep PBG gratings in the pulsed regime by directly integrating Maxwell's equations in the time domain.

Our results generally indicate that the enhancement mechanism that we predicted—and later demonstrated in PBG structures in the linear regime [6,38]—can lead to frequency up- (or down-) conversion rates nearly three orders of magnitude better than conversion rates achieved with ordinary phase matched materials, or in fiber grating geometries. The geometrical properties and the periodicity of the photonic “crystal” can act to significantly modify the density of electromagnetic field modes near the band edge, thus facilitating the emission of the SH signal at a much-enhanced rate. More importantly perhaps, this means that current fabrication issues that arise in ordinary quasi-phase-matched structures can be avoided altogether by utilizing current technology for deposition of semiconductor or dielectric thin films.

In our past work we emphasized pulse propagation and dynamics within the context of a small number of periods (15–30 in general), and large index contrast between layers (δn of order unity). This situation differs significantly from ordinary distributed feedback reflectors DFB's with small index modulation (thousands of periods and $\delta n \leq 10^{-3}$), in that ultrashort pulses can be transmitted through our PBG crystal with large retardation, and without any significant degradation, as theory and experiment clearly show [7]. In contrast, small-index-modulation DFB's (or shallow fiber gratings) can be highly dispersive, even for long pulses, leading to pulse broadening in the linear regime. In general, both PBG's and DFB's are geometrically similar. However, several physical characteristics are in fact very different, the most obvious being their physical lengths. Also, the bandwidths and features of both transmission resonances and band gaps are considerably larger for PBG structures than for ordinary DFB's.

Consideration of nonlinear effects can highlight even more dramatic differences. Typical nonlinear index changes in GaAs or AlAs layers can be of order $\delta n_{\text{NL}} \approx 10^{-3}$. This implies that nonlinear index shifts can be larger than the linear index modulation depth. Consequently, the location of the gap on the frequency axis can shift dramatically to higher or lower frequencies, and its bandwidth can increase or decrease significantly, depending on the sign of the nonlinearity. This effect is credited for the onset of pulse narrowing and solitonlike pulses of 25–60 ps in duration, which have recently been observed experimentally in a fiber grating [39]. The frequency bandwidth of such pulses can be much wider than the gap itself, and tuning the pulse near the band edge

causes considerable linear dispersion, as was recently shown [39]. Such dispersion is necessary for the observation of this solitonlike behavior.

In contrast, the frequency bandwidth of a pulse only a few hundred optical cycles in duration can be smaller (depending on the wavelength) than the bandwidth of the PBG's first transmission resonance peak, where the group velocity is a minimum. Here, ultrashort pulse propagation can be nondispersive, as our group has shown [7]. In addition, the nonlinear index change remains orders of magnitude smaller than the index modulation depth, which in our case can be of order unity or larger. Thus gap and transmission resonance bandwidths, and their locations, are only marginally altered, although changes may be sufficient for the onset of optical limiting and switching, optical diode behavior, and strong pulse reshaping [4–7].

The stability of the band structure in the frequency domain is also important in parametric optical up- and down-conversion, and harmonic generation, which is the subject of this paper. In small-index modulation DFB's [39], linear dispersion due to the grating structure, and shifts of the band gap due to nonlinear index changes, can lead to shifts of the frequency tuning of the pump with respect to the band edge. This effective detuning can cause an effective lowering of the cavity Q , a reduction of the pump intensity, and a decrease of SH gain. In a companion paper [40], analytical multiple-scale perturbation theory was used in order to analyze the small index modulation regime typical of fiber gratings. In that study, the authors showed that it may be possible to achieve 2–3 orders of magnitude SH enhancement for plane waves incident on mm-long, 20 000-period fiber Bragg gratings, whose index modulation is of order 5×10^{-3} . The pump frequency is assumed to be resonant with the photonic band-edge resonance; the SH signal was tuned in the middle of the pass band. The predicted SH gain enhancement is therefore solely attributed to pump intensity enhancement inside the grating. These results, when coupled with the present study, highlight the fact that a new generation of compact and efficient high gain optical amplifiers and optical parametric oscillators based on photonic band-edge effects may soon be realized.

In general, large index modulation PBG structures are not as easily susceptible to band-structure shifts due to nonlinear index changes ($\delta n_{\text{NL}} \approx 10^{-3}$) because index variations are a small perturbation on the linear index modulation depth. As we will see below, our calculations show that, for ultrashort pulses tuned near the photonic band edge, a choice of materials with suitable indices of refraction, thicknesses, and periodicity can lead to low group velocities, enhanced field intensity, and conversion efficiencies nearly three orders of magnitude larger than conventional bulk up-conversion rates. Conversion efficiencies greater than 10^{-3} are not uncommon for structures only a few micrometers in length, with a single pump pass, and at realistic pump intensities. Plane-wave conversion rates can be approximated by utilizing pulses whose frequency bandwidth is smaller than the transmission resonance bandwidth, in this case only a few ps in duration.

We point out that these conversion efficiencies can be even higher for structures with an increased number of periods. For example, we find that increasing the structure length by 50% (from 20 to 30 periods), the energy output can in-

crease by a factor of 5. The only limitations appear to be (a) the transmission resonance bandwidth decreases as $1/N^2$, where N is the number of periods, so that the pulse duration needs to be increased in order to ensure large pump enhancement inside the structure [41]; and (b) material breakdown may occur because of excessive electric-field buildup, or enhancement, inside the structure.

The reason for the enhancement of gain in these structures can be understood if we recall that the density of accessible field modes in the vicinity of dielectric boundaries is modified by the boundary conditions, as first indicated by Purcell [42]. Many experimental and theoretical investigations have confirmed this fact since Purcell's original prediction [43]. This means that if a linear or nonlinear gain medium is introduced within a PBG structure, the stimulated and spontaneous emission rates are modified according to Fermi's golden rule [38]. In quasi-phase-matched structures, a minimization of the phase difference between the waves is desirable in order to avoid a phase mismatch in the cw case. This is typically achieved by poling the active material—which is *uniform* in its composition and contains *no linear index discontinuities*—in such a way that the nonlinear coefficient only alternates sign in the longitudinal direction, every few tens of micrometers [13–29]. Here our approach departs significantly from convention. We rely on the unusually strong confinement of *both* the pump and the SH signal that occurs near the photonic band edges, where the density of electromagnetic field modes is large, the group velocity is low, the field amplitude may be enhanced over bulk values by one order of magnitude or more, and strong pump and SH mode overlap occurs. In this regime, the material is not poled in the usual manner; it is the geometrical properties of the structure that cause strong mode overlap, copropagation, and larger interaction times, the combination of which is ultimately responsible for the enhanced gain that we observe in our simulations.

II. MODEL

We consider the following simple one-dimensional system. The crystal is composed of 40 dielectric layers (20 periods in all, roughly $12 \mu\text{m}$ thick for a reference wavelength of $1 \mu\text{m}$), and the index of refraction alternates between a high and a low value, $n_2 = 1.42857$ (we chose this value for computational expediency), and $n_1 = 1$. We take a rather small value of $\chi^{(2)} \approx 0.1 \text{ pm/V}$ (roughly $3 \times 10^{-9} \text{ cm/statvolt}$ in Gaussian units) and assume that the nonlinear material is distributed uniformly throughout the PBG structure. Then, for a reference wavelength λ_0 , the layers have thicknesses $a = \lambda_0 / (4n_1)$ and $b = \lambda_0 / (2n_2)$, respectively. This forms a mixed half-quarter-wave stack for wavelength λ_0 . A range of frequencies is reflected, as shown in Fig. 1, where we plot the transmission coefficient for this structure as a function of the scaled frequency $\Omega = \omega / \omega_0$, where $\omega_0 = 2\pi c / \lambda_0$. The figure suggests that this choice of parameters causes the location of the second-order gap to be removed from the first-order gap by approximately a factor of 2. For an ordinary quarter-wave structure, a factor of 3 separates the first- and second-order band edges and based on our results, utilizing these two edges would be more appropriate for third-harmonic generation. The equations of motion can be de-

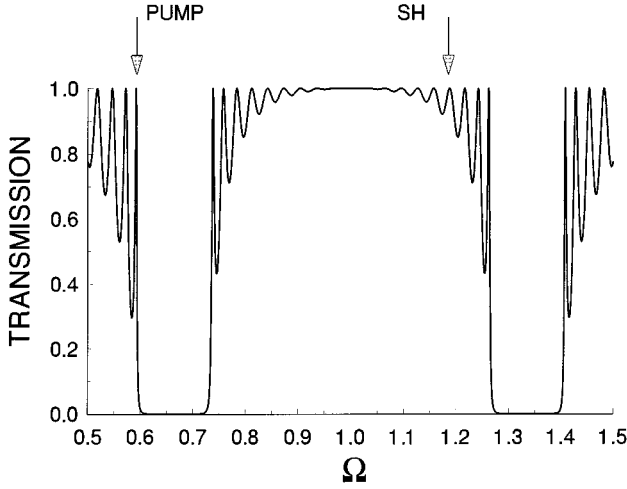


FIG. 1. Transmission vs normalized, dimensionless frequency for a 20-period, half-quarter-wave stack. The indices are $n_1 = 1$ and $n_2 = 1.42957$, and no dispersion is assumed. Tuning the pump at the low-frequency band edge causes the SH signal to be tuned away from the second-order, low-frequency band edge. The bandwidth of a picosecond pump pulse is narrower than the bandwidth of the first transmission resonance where the pump is tuned. In this case, the second harmonic signal is enhanced only slightly with respect to bulk due to the large detuning from the band edge.

rived beginning with Maxwell's equation for the total field, in Gaussian units, and can be written as

$$\frac{\partial^2}{\partial z^2} E(z,t) - \frac{n^2}{c^2} \frac{\partial^2}{\partial t^2} E(z,t) = \frac{4\pi}{c^2} \frac{\partial^2}{\partial t^2} P_{NL}. \quad (1)$$

Here, P_{NL} is the total nonlinear polarization. Without loss of generality, the fields can arbitrarily and conveniently be decomposed as follows:

$$E(z,t) = \mathcal{E}_\omega(z,t)e^{i(kz - \omega t)} + \text{c.c.} + \mathcal{E}_{2\omega}(z,t)e^{2i(kz - \omega t)} + \text{c.c.}, \quad (2)$$

$$P_{NL}(z,t) = \mathcal{P}_\omega(z,t)e^{i(kz - \omega t)} + \text{c.c.} + \mathcal{P}_{2\omega}(z,t)e^{2i(kz - \omega t)} + \text{c.c.} \quad (3)$$

This decomposition highlights the fundamental and second-harmonic angular frequencies. The nonlinear polarization can be expanded in powers of the electromagnetic field strength as follows:

$$P_{NL}(z,t) = \chi^{(2)} E^2(z,t) = 2\chi^{(2)} \mathcal{E}_\omega^*(z,t) \mathcal{E}_{2\omega}(z,t) e^{i(kz - \omega t)} + \text{c.c.} + \chi^{(2)} \mathcal{E}_\omega^2(z,t) e^{2i(kz - \omega t)} + \text{c.c.} \quad (4)$$

While we can assume an initial left- or right-propagating pump pulse, the SH signal is initially zero everywhere. The direction of propagation of the spontaneously generated SH field, and the exact nature of the quasistanding wave inside the structure, are dynamically determined by the nature of the initial and boundary conditions, pump-frequency tuning with respect to the band edge, and the distribution of nonlinear dipoles inside the structure. This nonlinear dipole distribution can significantly affect the results. SH generation is a phase-sensitive process; the field and its phase at any point inside the structure are a superposition of all fields originat-

ing everywhere else inside the structure, thus making phase an important element that must be included in the integration of the equations of motion. However, dipole distribution is important to the extent that it is modified in the layers where the fields happen to be localized. For instance, near the low-frequency band edges, the fields are localized in the high-index layers. Modifying the nonlinear medium distribution in the low-index layers will have little effect, although some mode overlap between layers always occurs. Our calculations bear this out.

Since we are considering ultrashort incident pulses propagating in the presence of large index discontinuities, we must retain all second-order spatial derivatives in order to properly include boundary conditions. However, we assume that pulse envelopes have a duration that is always much greater than the optical cycle, thus allowing the application of the slowly varying envelope approximation in time (SVEAT) only [4–7]. The equations of motion for the fundamental and the second-harmonic fields can be derived as follows. First, substituting Eq. (2) into Eq. (1) yields

$$\frac{\partial^2 \mathcal{E}_\omega}{\partial z^2} + 2ik \frac{\partial \mathcal{E}_\omega}{\partial z} - k^2 \mathcal{E}_\omega - \frac{n_\omega^2}{c^2} \frac{\partial^2 \mathcal{E}_\omega}{\partial t^2} + \frac{2i\omega n^2}{c^2} \frac{\partial \mathcal{E}_\omega}{\partial t} + \frac{\omega^2}{c^2} n_\omega^2 \mathcal{E}_\omega = \frac{4\pi}{c^2} \left(\frac{\partial^2}{\partial t^2} \mathcal{P}_\omega - 2i\omega \frac{\partial}{\partial t} \mathcal{P}_\omega - \omega^2 \mathcal{P}_\omega \right), \quad (5)$$

$$\begin{aligned} \frac{\partial^2 \mathcal{E}_{2\omega}}{\partial z^2} + 4ik \frac{\partial \mathcal{E}_{2\omega}}{\partial z} - 4k^2 \mathcal{E}_{2\omega} - \frac{n_{2\omega}^2}{c^2} \frac{\partial^2 \mathcal{E}_{2\omega}}{\partial t^2} \\ + \frac{4i\omega}{c^2} n_{2\omega}^2 \frac{\partial \mathcal{E}_{2\omega}}{\partial t} + 4 \frac{\omega^2}{c^2} n_{2\omega}^2 \mathcal{E}_{2\omega} \\ = \frac{4\pi}{c^2} \left(\frac{\partial^2}{\partial t^2} \mathcal{P}_{2\omega} - 4i\omega \frac{\partial}{\partial t} \mathcal{P}_{2\omega} - 4\omega^2 \mathcal{P}_{2\omega} \right). \end{aligned} \quad (6)$$

We now make the following assumptions: we choose $k = \omega/c$, and make the SVEAT only. This choice of wave vector is simply an initial condition consistent with a pump field of frequency ω initially propagating in free space, located away from any structure. Any phase modulation effects that ensue from propagation, i.e., reflections and nonlinear interactions, are accounted for in the dynamics of the field envelopes. The inclusion of all second-order spatial derivatives in the equations of motion means that reflections are accounted for to all orders, without any approximations. Details on the propagation method can be found in Refs. [4–7]. Therefore, assuming that pulses never become so short as to violate SVEAT (usually this means a few tens of optical cycles if propagation distances are on the order of pulse width), neglecting all but the lowest order temporal contributions to the dynamics, and using the nonlinear polarization expansions of Eqs. (4), Eqs. (5) and (6) become

$$\begin{aligned} n_\Omega^2 \dot{\varepsilon}_\Omega(\xi, \tau) = \frac{i}{4\pi\Omega} \frac{\partial^2 \varepsilon_\Omega}{\partial \xi^2} - \frac{\partial \varepsilon_\Omega}{\partial \xi} + i\pi(n_\Omega^2 - 1)\Omega \varepsilon_\Omega \\ + i8\pi^2 \Omega \chi^{(2)} \varepsilon_\Omega^* \varepsilon_{2\Omega}, \end{aligned} \quad (7)$$

$$n_{2\Omega}^2 \dot{\varepsilon}_{2\Omega}(\xi, \tau) = \frac{i}{8\pi\Omega} \frac{\partial^2 \varepsilon_{2\Omega}}{\partial \xi^2} - \frac{\partial \varepsilon_{2\Omega}}{\partial \xi} + i\pi(n_{2\Omega}^2 - 1)2\Omega \varepsilon_{2\Omega} + i8\pi^2\Omega \chi^{(2)} \varepsilon_{\Omega}^2. \quad (8)$$

Here $\xi = z/\lambda_0$, and $\tau = ct/\lambda_0$. The spatial coordinate z has been conveniently scaled in units of λ_0 ; the time is then expressed in units of the corresponding optical period. As we will see below, forward and backward SH generation can occur. If we assume that the medium is dispersionless, and the pump is tuned at the low-frequency band-edge transmission resonance, then the SH frequency is found well away from the second-order band edge. It is tuned in the middle of the pass band, as indicated in Fig. 1. In order to properly tune the SH signal frequency near the band edge, we introduce material dispersion. This causes changes in the band structure. Specifically, all higher-order gaps tend to move down in frequency, causing the SH signal to be tuned closer to the low-frequency, second-order band edge, where the electromagnetic density of states is largest.

From a calculational standpoint, varying the amount of dispersion is simplest to undertake. From a fabrication standpoint, obtaining the same conditions is clearly more difficult. However, we find that the band structure and its features are strongly influenced by (a) the number of periods, (b) layer thickness, and (c) material dispersion. For example, increasing (decreasing) the number of layers sharpens the band edges, and increases (decreases) the number of transmission resonances between gaps, causing an effective shift of each resonance [41]. Changing layer thickness away from the quarter- or half-wave conditions (in units of λ_0) can also cause frequency shifts in the location of the band gaps and transmission resonances. When these frequency shifts are coupled with material dispersion, a structure with the right properties may be realized. Later we will show that the conditions and results that we discuss below can be repeated for a 20-period GaAs/AlAs structure.

In order to find the optimal parameters for SH generation, i.e., tuning with respect to the band edge, we vary the index of refraction of the high-index layer from $n_2(2\Omega) = 1.42857$ to $n_2(2\Omega) = 1.65$. The higher-index value corresponds to SH generation just inside the second-order gap, where we expect its suppression. For intermediate values of the index, SH generation also occurs at frequencies where the density of modes is a maximum. The degree of dispersion that we assume is typical of the degree of dispersion found in both dielectric or semiconductor materials, 5–10% in this case.

Figure 2 shows the group index, defined as $N_g = cdk/d\omega$, for our sample [41]. (We note that the maximum group index is also a sensitive function of δn , the index modulation depth, and the number of periods. The maximum value of the group index for this mixed half-quarter-wave structure is similar in magnitude to that of a quarter-wave, 20-period structure with the same index modulation depth.) In this case, $n_2(\Omega) = 1.42857$, and $n_2(2\Omega) = 1.519$. Note that the magnitude of this function is largest near the high- and low-frequency band edges. We thus compare the SH generation from this device with a uniform index-matched (same index of refraction for pump and signal) bulk medium of similar dimensions, coated with antireflection layers at

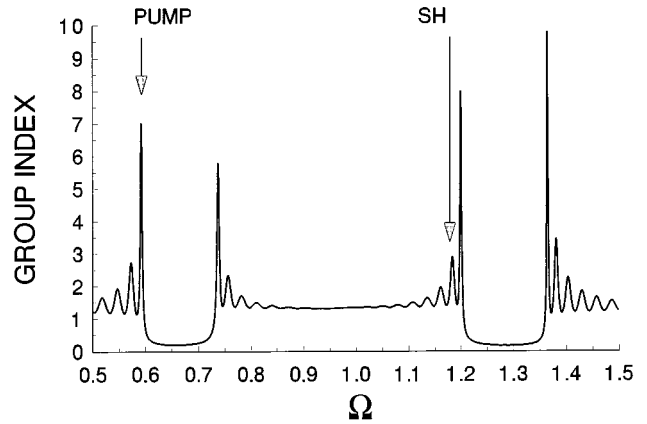


FIG. 2. Group index vs normalized, dimensionless frequency. This function also represents the electromagnetic density of modes, in units of c . There is just enough dispersion in the system to cause the SH signal to be tuned at the second resonance peak near the band edge, as indicated in the figure. The effect of normal dispersion, i.e., the index increases with frequency, is to shift the band structure to lower frequencies.

both ends to avoid cavity effects for the pump field, and compute conversion efficiencies for the periodic structure. We point out that the group-index maxima are directly correlated to the transmission maxima, a fact that was exploited in the design of the photonic band-edge delay line [7], and is clearly important for the onset of dramatically higher nonlinear gain.

III. DISCUSSION AND RESULTS

A. Generic model

We choose the carrier frequency of an incident pump pulse at the low-frequency band edge, where the transmission resonance is approximately unity and the group index is a maximum ($\Omega = 0.591$ in Fig. 2). A high pump index implies that a dramatic increase in the field intensities inside the structure occurs at that frequency. This is important, since SH gain is nonlinear in the field, as Eq. (8) suggests. When we choose the index of refraction such that $n_2(2\Omega) = 1.519$, the SH frequency coincides with the second density of modes maximum on the low-frequency side of the second-order band gap [see Fig. (2)]. Here, we find that for this structure the total-energy output from the PBG device with respect to the index-matched bulk, which includes forward and backward SH generation, varies from one order of magnitude for pump pulses only 60 optical cycles in duration ($1/e$ width of the intensity envelope is about 200 fs if $\lambda_0 = 1 \mu\text{m}$), to approximately 500 times for pulses roughly 1 ps long. For subpicosecond pulses, the enhancement is reduced due to the broad frequency content of the pulse.

We note that SH generation is not at a maximum when the SH signal is tuned at the density of the mode maximum, probably because the fields do not have the right phase for this to occur. As an example of the complexity of the system, using the matrix transfer method we find that the phase of the transmitted, plane-wave field undergoes a π phase shift across the gap, and a phase shift of 2π between consecutive resonances on the same side of any gap. Therefore, the num-

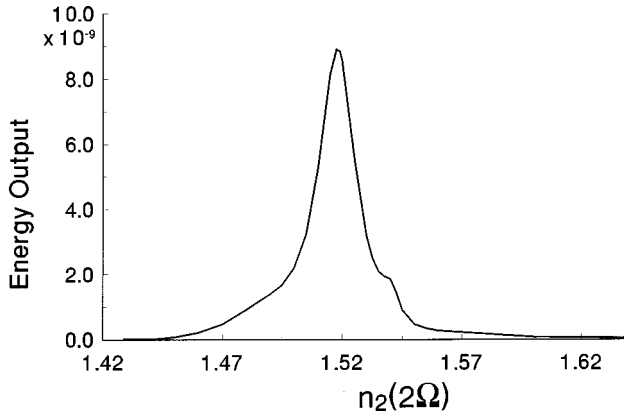


FIG. 3. Maximum energy output vs index of refraction. This plot is also representative of the dependence of SH energy on material dispersion. The maximum out occurs when the SH signal is tuned to the second resonance peak, as indicated on Fig. 2. The shoulder at $n_2 \approx 1.54$ corresponds to the first band-edge resonance. For $n_2 > 1.55$, the SH signal is suppressed by the band gap.

ber of periods chosen may have an impact on the overall phase of the SH field inside the structure. For short pulses, the circumstances are much more complicated, because of their broadband frequency make-up.

In Fig. 3 we show the calculated SH energy output for a ps pulse, as a function of $n_2(2\Omega)$, i.e., dispersion. The maximum energy output occurs when $n_2(2\Omega) = 1.519$, which corresponds to the second transmission or group index maximum. The band structure for $M_2 = 1.519$ is illustrated in Fig. 2. Evidence of the curvature of the band structure near the band edge is rather weak away from the second transmission resonance. As we mentioned earlier, the dipole distribution is an important factor that cannot be overstated, and certainly needs further investigation. In this case, we point out that the SH field is generated inside the structure from a continuous distribution of nonlinear dipoles; the nonlinearity is in both the high and low index layers. This dipole distribution determines the form of the propagating eigenmode, and the manner in which the generated signal leaves the structure. Therefore, it may be possible to find a nonlinear dipole distribution that will maximize or further improve SH conversion efficiency, although that is beyond the scope of this work.

In our calculations, we also highlight the importance of pulse width. Pulses whose spectral widths are larger than the band-edge transmission resonance tend to couple poorly with the structure. This situation leads to dispersive propagation, and to only slightly enhanced field intensities inside the PBG structure. On the other hand, a pulse whose frequency bandwidth is smaller than the band-edge resonance bandwidth has fewer frequency components, experiences little or no dispersion, and allows the field to build up inside the structure by about one order of magnitude or more with respect to its free space or bulk values, where the field amplitude is in general proportional to E_{free}/n . In Fig. 4(a) we plot the pump-field intensity inside the structure, at the instant the peak of the 1-ps pulse reaches the structure. This intensity is enhanced by more than one order of magnitude compared to its peak value outside the structure. Figure 4(b), on the other hand, represents the SH field intensity quasistanding-wave pattern at the same instant in time as Fig. 4(a). Both eigenmodes

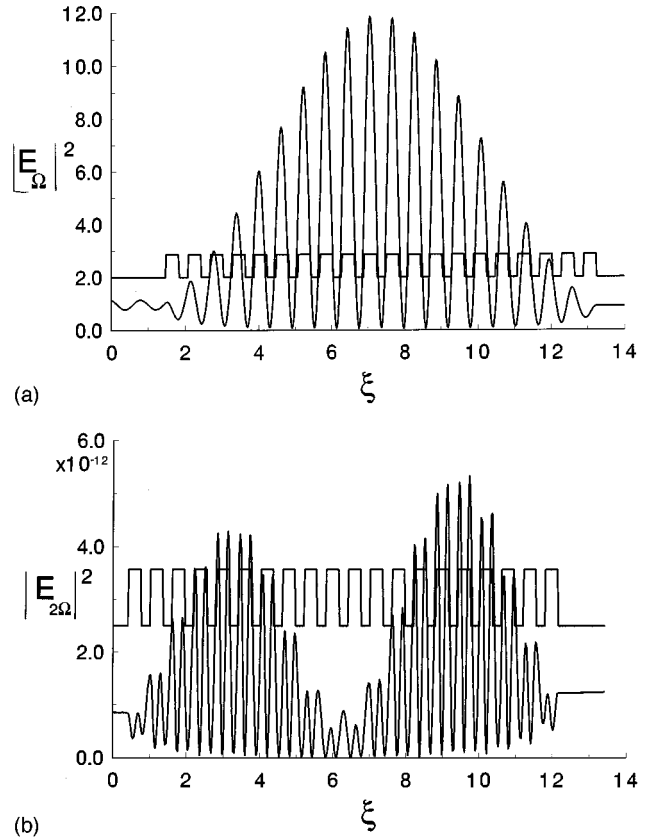


FIG. 4. (a) Pump field eigenmode distribution inside the structure, at the instant that the peak of the pulse reaches the structure. As the pulse slows down dramatically, the maximum field intensity is amplified by more than one order of magnitude by linear interference effects of backward- and forward-traveling components. Pump pulse depletion is negligible, and more than 90% transmission occurs in this case. In view of the magnitude of the field intensity, the SH eigenmode overlaps extremely well with the pump eigenmode. (b) Second-harmonic eigenmode for the case of (a). The fact that two envelopes can be identified inside the structure is due to the fact that the SH signal is tuned to the second resonance away from the band edge. The fact that there are two maxima inside each high index layer, in contrast to the pump single peak, is due to the fact that the wavelength of the SH signal is half that of the pump.

overlap to a large extent inside the high index layers, and the fields propagate in this configuration for the entire duration of the pump pulse. This mode overlap, combined with the dramatic group velocity reduction for both fields, allows efficient energy exchange between the pump and the SH signal.

In Fig. 5 we plot the total-energy output (forward and backward included) as a function of incident pulse width, expressed in optical cycles, for a 20-period, 12- μm -thick device (solid line), and a 12- μm bulk sample coated with anti-reflection layers at both ends to minimize pump reflections (dotted line). We consider low input field intensities that yield conversion efficiencies on the order of 10^{-12} , although this trend persists as long as pump depletion is not significant. For clarity, the abscissa is plotted on a logarithmic scale. The figure shows that the total-energy output (and therefore power output) becomes about 500 times greater for

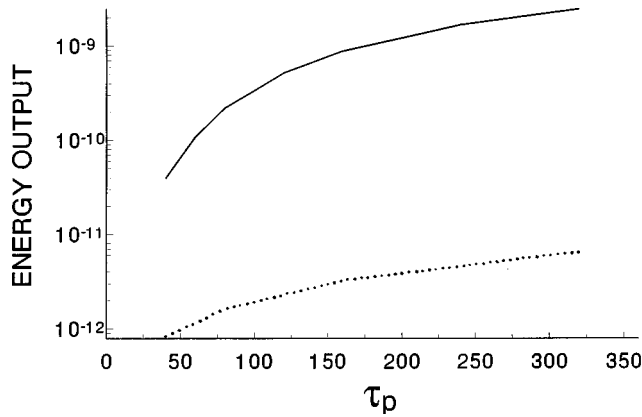


FIG. 5. Comparison between the SH energy output from the PBG (solid line) and a phase-matched bulk material (dotted line), as a function of pulse width. The y axis is represented in a logarithmic scale. The pulse width is given in units of the optical cycle, as described in the text. The output from the PBG structure is about 500 times greater than the bulk material output when the incident pulse width approaches 300 optical cycles, or about 1 ps.

the PBG sample than for index-matched bulk when pulse width approaches 300 optical cycles, or about 1 ps. Our results indicate that at these length scales the energy output for the bulk sample increases linearly with incident pulse width. In contrast, an early exponential increase characterizes energy growth in the PBG case, giving way to linear growth only when pulse width approaches 1 ps. This implies that the pump field eigenmode intensity (and hence SH gain) increases rapidly with pulse width, saturating when a quasimonochromatic limit is reached, in this case, when pulse frequency bandwidth is somewhat less than band-edge resonance bandwidth. We also point out that both the amplitude and the width of the generated SH pulses increase with increasing incident pulse width. Figure 6 shows the SH field propagating away from the structure; While the pump was incident from the left, note that the structure radiates significantly in both directions, and that the SH pulses generated have the same width as incident pump pulses; it would be difficult to predict this overall behavior *a priori*, especially in the absence of analytical results in this regime. We also point out that tuning the pump away from the band edge, tuning to the high-frequency band edge, or modifying the nonlinear dipole distribution can significantly alter the pattern of Fig. 6.

Figure 7 is a plot of the conversion efficiency vs peak field intensity in Gaussian units, for a pulse of ps duration ($|E|^2$ of 10^9 in these units corresponds to roughly 10 GW/cm^2 in free space. The free-space value of the energy flow is to be distinguished from energy flow inside the structure. As we pointed out in previous publications [7,44], the notions of energy, energy density, and Poynting vector are significantly modified inside the structure). We define efficiency as the ratio between the final total SH energy and the total initial pump energy. This ratio is also representative of the ratio between the corresponding peak field intensities, respectively. The figure suggests that for this simple structure only $12 \mu\text{m}$ in length, a conversion efficiency of order 10^{-2} could be achieved with pump intensity of 10 GW/cm^2 , yielding a SH signal intensity of approximately 100 MW/cm^2 . This is quite dramatic and remarkable, consider-

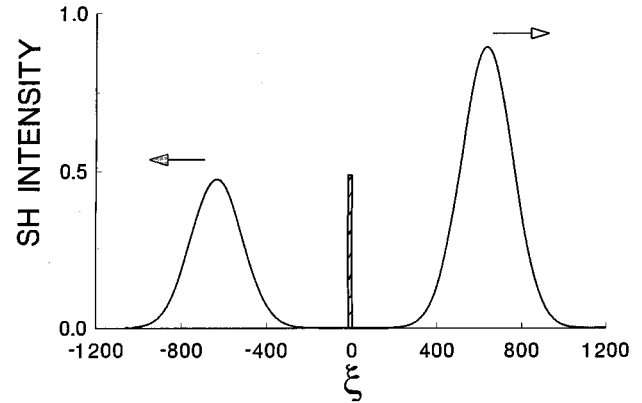


FIG. 6. Spontaneously generated SH pulses. The amplitude has been normalized to unity without loss of generality. The structure is about $12 \mu\text{m}$ in length, and is located near the origin. The width of the scattered pulses is roughly the same as the width of the incident pump pulse. However, the maximum amplitude of each pulse increases with the incident pulse width, until the quasimonochromatic limit is reached (about 1 ps in this case).

ing that our structure is only a few micrometers in length, only a single pump pass occurs, and that we are using a very modest value of $\chi^{(2)} \approx 0.1 \text{ pm/V}$. Considering the extremely compact nature of our device, and that the pump traverses the sample only once, the gain-to-device length ratio undergoes several orders of magnitude improvement over current state of the art devices.

We now provide a simple physical argument that will help us understand the reason for such large enhancements with respect to phase-matched up-conversion. According to Fermi's golden rule, the power radiating from an oscillating dipole is given by $P(\omega) = \rho(\omega) |E(\omega)|^2$, where $\rho(\omega)$ is the density of modes and $|E(\omega)|^2$ is the eigenmode intensity. The average energy output can be obtained by multiplying the power output by τ , the interaction time. As we have already pointed out, all these quantities increase by nearly one order of magnitude for our structure. In fact, since $|E(\omega)|^2$ and τ are both proportional to $\rho(\omega)$, then the total

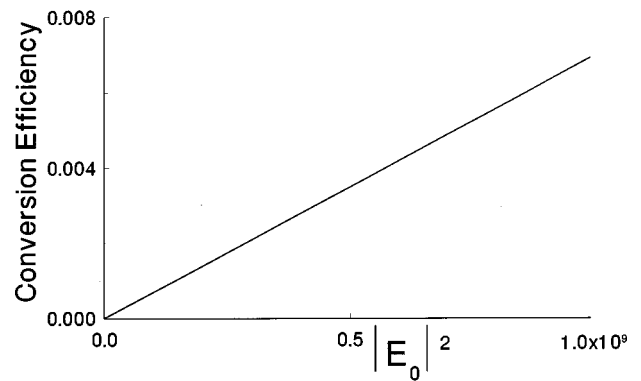


FIG. 7. SH conversion efficiency vs incident pulse peak field strength. As we noted in the text, an intensity of 10^9 corresponds to a free-space energy flow of about 10 GW/cm^2 . Our calculations indicate that the energy output, and hence conversion efficiency, is proportional to the number of pump passes inside the structure. We emphasize that the results we have discussed represent a single pass inside a PBG structure.

energy emitted is generally proportional to $\rho(\omega)^3$. Hence the significant increase in the total energy output that we report in Fig. 5.

We point out that higher conversion efficiencies can easily be achieved by increasing pump power, or, as we mentioned earlier, by increasing the length of the structure by only modest amounts. For example, our calculations show that by increasing the total number of periods to 30, thus increasing the length of the device by 50%, the SH output energy (and power level) increases by a factor of 5 for a ps pulse, enhancing the conversion efficiency by the same factor. This occurs because the maximum group index increases approximately as N^2 [41], where N is the number of periods. The field eigenmode intensity is also proportional to N^2 , thus enhancing energy output in a nonlinear fashion with respect to device length.

Our calculations also indicate that in the linear, undepleted-pump regime, the conversion efficiency is proportional to the free-space peak field value, as Fig. 7 shows. We point out that any small deviation in the actual $\chi^{(2)}$ value, tuning with respect to the band edge, and input pulse width could significantly affect comparison with experimental results. For this reason, the generic model is of great value in order to determine the overall behavior of the system, and it could also be used in the very determination of $\chi^{(2)}$. Therefore, exercising some care in the design process could produce a very efficient SH generator, provided absorption can be kept at bay.

Our discussion so far has been directed toward understanding pulse dynamics when the pump is tuned at the low-frequency band edge. However, we expect the same qualitative results to hold when the same analysis is applied to the high-frequency band edge. Generally, however, the half-quarter-wave structure discussed above does not lend itself to this task because tuning the pump at the high-frequency band edge results in a second harmonic frequency tuned well away from the band edge. We therefore consider a structure whose indices of refraction are as in Sec. II, i.e., $n_1(\Omega, 2\Omega) = 1$ and $n_2(\Omega, 2\Omega) = 1.42857$. For added simplicity, we assumed that the material is not dispersive. If layer thicknesses are chosen such that the width of the low index layer is $a = 0.65\lambda_0/n_1$ (the low index layer is now the active layer because of the shift in localization of the field), and the width of the high index layer is such that $b = 0.089\lambda_0/n_2$, then, tuning the pump at the first resonance of the first-order, high-frequency band edge causes the SH signal to be tuned at the second resonance of the second-order high-frequency band edge, in analogy to what was accomplished for the low-frequency band edge. Our simulations suggest that the results are qualitatively similar to those of Sec. II; we find, however, that the conversion efficiency can increase up to about a factor of 2 for ps pulses, compared to the low-frequency band-edge conversion efficiency. This increase can be understood with the following argument. Tuning the pump at the high-frequency band edge causes a shift of the pump field localization in the low index layer. This shift increases the field eigenmode intensity in that layer. Also, the width of the active layer increases by about 30%, from $0.5\lambda_0$ to $0.65\lambda_0$. This combination can account for the increase in overall nonlinear gain.

Clearly, then, there may be circumstances where the new geometry is to be preferred over that of the half-quarter-wave

stack since the new structure is still about $12\ \mu\text{m}$ in length, even though the output energy can increase by a factor of 2. However, we will not dwell on this point here, and simply point out that our calculations suggest that higher conversion efficiencies could be obtained by judiciously choosing the appropriate parameters.

B. GaAs/AlAs half-quarter-wave stack

We tested our numerical model with the parameters of a mixed half-quarter-wave structure composed of 20 periods of GaAs/AlAs material. In this case, we assumed $\chi^{(2)} \approx 1\ \text{pm/V}$ for both materials, and the index of refraction alternates between $n_1(\Omega) = 2.868$ and $n_2(\Omega) = 3.31$, and $n_1(2\Omega) = 2.9$ and $n_2(2\Omega) = 3.35$ [45]. This occurs at frequencies well below the electronic band gaps of both materials, where absorption can be ignored. These indices correspond to a pump wavelength of $3\ \mu\text{m}$, and a second-harmonic signal at $1.5\ \mu\text{m}$. The results are in essence the same as to what we find in the generic model. This is because the parameters that we use combine to give approximately the same dynamic, nonlinear SH gain, which from Eq. (6) we define as the product $\chi^{(2)}\epsilon_\Omega^2$; the order-of-magnitude increase in $\chi^{(2)}$, and the order-of-magnitude decrease in the field eigenmode intensity (due to the substantial increase in the index for GaAs) produce conversion efficiencies that are also on the order $10^{-2} - 10^{-3}$ for this 20-period structure at a pump intensity of $10\ \text{GW/cm}^2$. We expect a significant increase with increasing number of periods.

We note that while it would be ideal to up-convert at higher frequencies, we could not find a set of parameters that allowed for that to occur in the GaAs/AlAs structure (mostly due to the large dispersion at higher frequencies), although our efforts were very limited in this regard; different materials, such as II-VI based semiconductors, may be necessary in order to achieve the enhancements that we have discussed. However, the fact that simple semiconductor structures appear to be useful for efficient SH generation, or frequency halving, where the dynamics and the role of pump and signal are reversed, is an encouraging development, since semiconductors periodic structures are simple to grow with well-established techniques.

IV. CONCLUSIONS

In summary, we discussed a novel SH generator based on a PBG, mixed half-quarter-wave, periodic structure. Both energy output and conversion efficiencies are nearly three orders of magnitude greater than for bulk, phase-matched devices of comparable lengths. We find similar results for a GaAs/AlAs semiconductor periodic structure. These results have immediate applications in frequency up- and downconversion lasers, higher and lower harmonic generation, and Raman-type lasers, where either Stokes or anti-Stokes resonances can be enhanced or suppressed near the band edge. In general, the underlying mechanism requires the fields to be strongly confined, allowing for longer interaction times, increased effective gain lengths, and enhanced conversion efficiencies, although strong pump confinement alone can also result in significantly enhanced SH generation.

- [1] E. Yablonovitch, *Phys. Rev. Lett.* **58**, 2169 (1987).
- [2] *Development and Applications of Photonic Band Gap Materials*, edited by C. M. Bowden, J. P. Dowling, and H. O. Everitt, special issue of *J. Opt. Soc. Am. B* **10**, 279–413 (1993); also, *Photonic Band Structures*, edited by G. Kurizki and J. W. Haus, special issue of *J. Mod. Opt.* **41** (1994).
- [3] C. Kittel, *Introduction to Solid State Physics*, 5th ed. (Wiley, New York, 1976), pp. 188 and 189.
- [4] M. Scalora, J. P. Dowling, C. M. Bowden, and M. J. Bloemer, *Phys. Rev. Lett.* **73**, 1368 (1994).
- [5] M. Scalora, J. P. Dowling, C. M. Bowden, and M. J. Bloemer, *J. Appl. Phys.* **76**, 2023 (1994); M. D. Tocci, M. J. Bloemer, M. Scalora, J. P. Dowling, and C. M. Bowden, *ibid.* **66**, 2324 (1995).
- [6] J. P. Dowling, M. Scalora, M. J. Bloemer, and C. M. Bowden, *J. Appl. Phys.* **75**, 1896 (1994).
- [7] M. Scalora, R. J. Flynn, S. B. Reinhardt, R. L. Fork, M. J. Bloemer, M. D. Tocci, J. Bendickson, H. Ledbetter, C. M. Bowden, J. P. Dowling, and R. P. Leavitt, *Phys. Rev. E* **54**, 2799 (1996).
- [8] J. He and M. Cada, *IEEE J. Quantum Electron.* **27**, 1182 (1991); N. D. Sankey, D. F. Prelewitz, and T. G. Brown, *Appl. Phys. Lett.* **60**, 1427 (1992); J. He, M. Cada, and M. A. Dupertuis, *J. Appl. Phys.* **63**, 866 (1993), and references therein; W. Chen and D. L. Mills, *Phys. Rev. Lett.* **58**, 2169 (1987); C. M. de Sterke and J. Sipe, *Phys. Rev. A* **38**, 5149 (1988); D. N. Christodoulis and R. I. Joseph, *Phys. Rev. Lett.* **62**, 1746 (1989); A. Kozhokin and G. Kurizki, *ibid.* **74**, 5020 (1995).
- [9] E. Yablonovitch *et al.*, *Phys. Rev. Lett.* **29**, 865 (1972); C. Flytzanis and N. Bloembergen, *Prog. Quantum Electron.* **4**, 271 (1974).
- [10] J. R. De Salvo, D. J. Hagan, M. Sheik-Bahae, G. Stegeman, E. W. Van Stryland, and H. Vanherzeele, *Opt. Lett.* **17**, 28 (1992); N. R. Belashenkov *et al.*, *Opt. Spectrosc.* **66**, 806 (1989).
- [11] G. I. Stegeman, M. Sheik-Bahae, E. Van Stryland, and G. Assanto, *Opt. Lett.* **18**, 13 (1993).
- [12] M. M. Fejer, *Phys. Today* **47**, 25 (1994).
- [13] A. Otomo, G. I. Stegeman, W. H. G. Horsthuis, and R. Muhlmann, *Appl. Phys. Lett.* **68**, 3683 (1996); F. Armani-Leplinger, J. J. Kingston, and D. K. Fork, *ibid.* **68**, 3695 (1996); V. Krylov, A. Rebane, A. G. Kalintsev, H. Schwoerer, and U. P. Wild, *Opt. Lett.* **20**, 198 (1995).
- [14] V. P. Yanovsky and F. W. Wise, *Opt. Lett.* **19**, 1952 (1994).
- [15] K. Yamamoto, K. Mizuuchi, Y. Kitaoka, and M. Kato, *Opt. Lett.* **20**, 273 (1995).
- [16] G. T. Moore, K. Koch, and E. C. Cheung, *Opt. Commun.* **113**, 463 (1995); E. C. Cheung, K. Koch, and G. T. Moore, *Opt. Lett.* **19**, 1967 (1994).
- [17] M. L. Bortz, M. A. Arbore, and M. M. Fejer, *Opt. Lett.* **20**, 49 (1995); L. E. Myers, G. D. Miller, R. C. Eckardt, M. M. Fejer, R. L. Byer, and W. R. Rosemberg, *ibid.* **20**, 52 (1995).
- [18] H. R. Jensen, *J. Opt. Soc. Am. B* **11**, 2359 (1994).
- [19] D. Blanc, A. M. Bouchoux, C. Plumereau, A. Cachard, and J. F. Roux, *Appl. Phys. Lett.* **66**, 659 (1995).
- [20] S. Kubodera, K. Midorikawa, H. Tashiro, and K. Toyoda, *Appl. Phys. Lett.* **66**, 133 (1995).
- [21] C. W. van Hasselt, M. A. C. Devillers, Th. Rasing, and O. A. Aktsipetrov, *J. Opt. Soc. Am. B* **12**, 33 (1995).
- [22] J. J. Zondy, M. Abed, and S. Khodja, *J. Opt. Soc. Am. B* **11**, 2368 (1994).
- [23] G. Assanto, G. Stegeman, M. Sheik-Bahae, and E. Van Stryland, *Appl. Phys. Lett.* **62**, 1323 (1993).
- [24] D. J. Hagan, Z. Wang, G. Stegeman, E. Van Stryland, M. Sheik-Bahae, and G. Assanto, *Opt. Lett.* **17**, 1305 (1994).
- [25] M. L. Sundheimer, Ch. Bosshard, E. W. Van Stryland, G. I. Stegeman, and J. D. Bierlein, *Opt. Lett.* **18**, 1397 (1993).
- [26] H. H. Zenzie and Y. Isyanova, *Opt. Lett.* **20**, 169 (1995).
- [27] G. Y. Wang and E. Garmire, *Opt. Lett.* **20**, 264 (1995); C. Y. Chien, G. Korn, J. S. Coe, J. Squier, G. Mourou, and R. S. Craxton, *ibid.* **20**, 353 (1995).
- [28] N. Bloembergen and A. J. Sievers, *Appl. Phys. Lett.* **17**, 483 (1970).
- [29] M. J. Steel and C. M. de Sterke, *Appl. Opt.* **35**, 3211 (1996).
- [30] J. Martorell and R. Corbalan, *Opt. Commun.* **108**, 319 (1994).
- [31] J. Trull, R. Valesca, J. Martorell, and R. Corbalan, *Opt. Lett.* **20**, 1746 (1995).
- [32] A. Yariv and P. Yeh, *J. Opt. Soc. Am.* **67**, 438 (1977).
- [33] J. P. van Der Ziel and M. Ilegems, *Appl. Phys. Lett.* **28**, 437 (1976).
- [34] S. Nakagawa, N. Yamada, N. Mikoshiba, and D. E. Mars, *Appl. Phys. Lett.* **66**, 2159 (1995).
- [35] D. S. Bethune, *J. Opt. Soc. Am. B* **6**, 910 (1989); **8**, 367 (1991).
- [36] N. Hashizume, M. Ohashi, T. Kondo, and R. Ito, *J. Opt. Soc. Am. B* **12**, 1894 (1995).
- [37] J. E. Sipe, *Surf. Sci.* **84**, 75 (1979); *J. Opt. Soc. Am. B* **4**, 481 (1987).
- [38] M. D. Tocci, M. J. Bloemer, M. Scalora, J. P. Dowling, and C. M. Bowden, *Phys. Rev. A* **53**, 2799 (1996); M. Scalora, J. P. Dowling, M. D. Tocci, M. J. Bloemer, C. M. Bowden, and J. W. Haus, *Appl. Phys. B* **60**, S57 (1995); J. P. Dowling and C. M. Bowden, *Phys. Rev. A* **46**, 612 (1992).
- [39] U. Mohideen, R. E. Slusher, V. Mizrakhi, M. K. Gonokami, P. J. Lemaire, J. E. Sipe, C. M. de Sterke, and N. G. R. Broderick, *Opt. Lett.* **20**, 1674 (1995); B. J. Eggleton, R. E. Slusher, C. M. de Sterke, P. A. Krug, and J. E. Sipe, *Phys. Rev. Lett.* **76**, 1627 (1996).
- [40] J. W. Haus *et al.* (unpublished).
- [41] J. M. Bendickson, J. P. Dowling, and M. Scalora, *Phys. Rev. E* **53**, 4107 (1996).
- [42] E. M. Purcell, *Phys. Rev. A* **69**, 681 (1946).
- [43] See, for example R. G. Hulet, E. S. Hilfer, and D. Kleppner, *Phys. Rev. Lett.* **55**, 67 (1992); D. Meschede, H. Walther, and G. Muller, *ibid.* **54**, 551 (1985); M. D. Tocci, M. J. Bloemer, M. Scalora, J. P. Dowling, and C. M. Bowden, *Phys. Rev. A* **53**, 2799 (1996).
- [44] M. Scalora, J. P. Dowling, A. S. Manka, C. M. Bowden, and J. W. Haus, *Phys. Rev. A* **52**, 726 (1995).
- [45] *Handbook of Optical Constants*, edited by E. D. Palik (Academic, New York, 1985).